

Controlling the lateral displacement of building with external lever by using of MR damper

Kambiz Takin^{*1}, Behrokh Hosseini Hashemi^{2a} and Masoud Nekooei^{3b}

¹Department of Civil Engineering, Safadasht Branch, Islamic Azad University, Tehran, Iran

²Structural Engineering Research Center (SERC), International Institute of Earthquake Engineering & Seismology (IIEES), Tehran, Iran, Member of IEAA

³Department of Civil Engineering, Science and Research Branch, Islamic Azad University, Tehran, Iran

(Received December 12, 2015, Revised June 25, 2017, Accepted June 26, 2017)

Abstract. This article is all about using the MR damper with an external lever system for mitigation torsional and transitional lateral displacements by using of PID control algorithm. The torsional modes are so destructive and can be varied during an earthquake therefore, using a semi-active control system mostly recommended for them. In this paper the corner lateral displacement of each floor obtains and then it equivalents in a solid member and it connects to an MR damper, which relies to a rigid structure to reduce the response. An MR damper is a semi-active control system, which can absorb a lot of energy by injecting current to it. This amount of current is very low and needs low power supply, but it increases the amount of damper force, rather than inactive systems like viscous dampers. This paper will show the appropriate algorithm for current injection into MR damper when the eccentricity of the load is changed by using of Bouc-Wen and Bingham's methods and illustrates the coincidence of them.

Keywords: MR damper; semi-active control system; torsion; Bingham model; Bouc-Wen model

1. Introduction

Due to an earthquake, so many buildings suffered severe damages, which were attributed to the torsional effect caused by eccentricity of load. Due to this type of torsional moments are generated, which are imposed by means of additional lateral forces developed at the resisting structural elements of the buildings (Stathi *et al.* 2015). The effect of torsion is being considered in seismic codes by the provision of design eccentricity of load where the static to dynamic eccentricity ratio is a parameter (Kamatchi *et al.* 2015). The reinforcement of torsional behavior structure against seismic and wind forces is the main purpose in structural designing (Nawy 2008, Saari *et al.* 2004). Therefore, the lateral bearing system in structure which has significant importance and the most considerable matter for the lateral displacement control (Park *et al.* 2007, Ellingwood *et al.* 2001). Damping is one of the main parameters, which control the performance of structures when they are subjected to seismic load. By adding supplemental viscous dampers, the energy input is absorbed, not only by the structure itself, but also by the supplemental dampers (Serror *et al.* 2014). Equip a building

with conventional lateral bearing systems may count for our needs, and they are able to bear against lateral forces such as wind and earthquake loads (Paulay 2002, Fintel 1974). Controlling these lateral forces gained through the shear wall for reinforced concrete structures and by the bracing for steel structures (Elgaaly 1998, Pall *et al.* 1996, Tong *et al.* 2005). One of the most common kinds of these systems is dual ones with moment resisting frame (M.R.F.) plus shear wall or steel bracing (Pettinga and Priestley 2005). The buildings with various shaped plans which built as a unit; huge forces may accrue at the intersection of the arms (Tande and Patil 2013). The steel bracing system is one of the operational members, which can be used for buildings. The Steel bracing decreases the flexure and shear deformation and the story drifts (Kevadkar and Kodag 2013). The asymmetric shape of the structure results in a coupling of the transitional and rotational modes in building and movement of the foundation due to an earthquake. The torsional modes are one of the main damages, which caused during the earthquakes. The Michoacán Earthquake in Mexico, 1985, illustrated the importance of torsional deflections (Rosenblueth and Meli 1985, Crisafulli *et al.* 2004). Crisafulli (2004) conducted a huge investigation in the asymmetric structures, which analyzed by using static linear analysis and applying usual torsional provisions. The Crisafulli's researches confirmed conclusions and illustrated that the application of these provisions originates an increase of the lateral resistance of the structure, with uncertain effectiveness in the inelastic range to control the torsional modes. Another criterion to show the torsional mode is based on the using of eccentricities of load to equate the maximum drift, which obtained from dynamic

*Corresponding author, Ph.D.

E-mail: omran@engineer.com

^aPh.D.

E-mail: behrokh_h_h@yahoo.com

^bPh.D.

E-mail: msnekooei@gmail.com

and static analyses (Tso and Moghaddam 1998, Calderoni *et al.* 2002). The development of softwares for analyzing and designing of structures allow performing an exact response from dynamic analysis (Crisafulli *et al.* 2004). The parameters of PID controller are found by using of a numerical algorithm, which considering time delay, maximum allowed control force and time domain analyses of shear buildings under different earthquake excitations (Nigdeli 2014).

The MR damper just looks like a simple viscous damper, but inside of it is filled with a special fluid that contains small polarizable particles. This device can provide reliability for uncontrolled systems and requires low power supply than active control devices. The semi-active control device is a trustworthy system with a higher reliability. The fluid inside the MR damper can be transitioned from semi-solid to be liquid by magnetic field, which produced by the copper coil surrounding the piston. The liquid's yield strength relates to the applied current (Nawy 2008, Saari 2004, Park *et al.* 2007). There are different kinds of semi-active control devices such as, dampers with controllable fluid, dampers with variable orifice and friction. These devices have been more attractive because they are so reliable and operated by low power. The semi-active control system is defined as a device that has constant mechanical energy but its dynamic properties can be varied. This semi-active control system is adaptable and expected to be effective for structural response reduction. Therefore, unlike its active ones, this system does not require huge power. So, these systems are inherently stable, which result in appropriate performances for structural response reduction (Dyke *et al.* 1996, 1997). The possibility of using this system as a vibrationally control system performed by different controller algorithm in buildings and many researchers have studied the behavior of structures with MR dampers (Tsang *et al.* 2006). Most of these studies could not be applicable to real size of structures because they are using small-scale MR dampers. Spencer *et al.*, performed an investigation about this system based on Bouc-Wen hysteresis model. This hysteric model was used for demonstrate the performance of this device (Dyke *et al.* 1996a, b, c, d). After that, he developed his model by using this device to control a multi-story structure (Dyke and Spencer 1997) and also a large-scale 20-tons MR damper is being tested in the university of Notre Dame (Spencer *et al.* 1997b, Carlson and Spencer 1996b).

2. The stiffness and mass matrices of a torsion-shear building

The centers of stiffness and mass are identified as C.R. and C.M. These matrices can be calculated based on the C.R. and C.M. points. The easiest way is to consider the C.M. point, so, the stiffness matrix determines based on the distance between the C.R. and C.M., but the mass matrix remains diagonal. For one, two and three-story buildings, the stiffness and mass matrices in a building with rigid floor(s) eventually obtained, as show in Eqs. (1)-(3). The diagonal mass matrices for one, two and three-story buildings with

torsional behavior obtain from Eqs. (4)-(6). The mass and stiffness matrices can be expanded for n-floor building. (Legzian and Hosseini 2011)

$$[K] = \begin{bmatrix} K_x & 0 & -K_x e_y \\ 0 & K_y & K_y e_x \\ -K_x e_y & K_y e_x & K_\theta + K_x e_y^2 + K_y e_x^2 \end{bmatrix} \quad (1)$$

$$[K] = \begin{bmatrix} K_{x1}+K_{x2} & 0 & -K_{x1}e_{y1}-K_{x2}e_{y12} & -K_{x2} & 0 & K_{x2}e_{y2} \\ 0 & K_{y1}+K_{y2} & K_{y1}e_{x1}+K_{y2}e_{x12} & 0 & -K_{y2} & -K_{y2}e_{x2} \\ & & K_{\theta11}+K_{x1}e_{y1}^2 & & & -(K_{\theta22}+K_{x2}e_{y2}^2) \\ -K_{x1}e_{y1} & K_{y1}e_{x1} & +K_{y1}e_{x1}^2+K_{\theta22} & K_{x2}e_{y12} & -K_{y2}e_{x12} & +K_{y2}e_{x2}^2+K_{x2}e_{y2}\Delta y \\ -K_{x2}e_{y12} & +K_{y2}e_{x12} & +K_{x2}e_{y12}^2+K_{y2}e_{x12}^2 & & & +K_{y2}e_{x2}\Delta x \\ -K_{x2} & 0 & K_{x2}e_{y12} & K_{x2} & 0 & -K_{x2}e_{y2} \\ 0 & -K_{y2} & -K_{y2}e_{x12} & 0 & K_{y2} & K_{y2}e_{x2} \\ & & -(K_{\theta22}+K_{x2}e_{y2}^2) & & & \\ K_{x2}e_{y2} & -K_{y2}e_{x2} & +K_{y2}e_{x2}^2+K_{x2}e_{y2}\Delta y & -K_{x2}e_{y2} & K_{y2}e_{x2} & K_{\theta22}+K_{x2}e_{y2}^2 \\ & & +K_{y2}e_{x2}\Delta x & & & +K_{y2}e_{x2}^2 \end{bmatrix} \quad (2)$$

$$[K] = \begin{bmatrix} K_{11} & K_{12} & K_{13} & K_{14} & K_{15} & K_{16} & K_{17} & K_{18} & K_{19} \\ K_{21} & K_{22} & K_{23} & K_{24} & K_{25} & K_{26} & K_{27} & K_{28} & K_{29} \\ K_{31} & K_{32} & K_{33} & K_{34} & K_{35} & K_{36} & K_{37} & K_{38} & K_{39} \\ K_{41} & K_{42} & K_{43} & K_{44} & K_{45} & K_{46} & K_{47} & K_{48} & K_{49} \\ K_{51} & K_{52} & K_{53} & K_{54} & K_{55} & K_{56} & K_{57} & K_{58} & K_{59} \\ K_{61} & K_{62} & K_{63} & K_{64} & K_{65} & K_{66} & K_{67} & K_{68} & K_{69} \\ K_{71} & K_{72} & K_{73} & K_{74} & K_{75} & K_{76} & K_{77} & K_{78} & K_{79} \\ K_{81} & K_{82} & K_{83} & K_{84} & K_{85} & K_{86} & K_{87} & K_{88} & K_{89} \\ K_{91} & K_{92} & K_{93} & K_{94} & K_{95} & K_{96} & K_{97} & K_{98} & K_{99} \end{bmatrix} \quad (3)$$

$$[M] = \begin{bmatrix} M_x & 0 & 0 \\ 0 & M_y & 0 \\ 0 & 0 & M_\theta \end{bmatrix} \quad (4)$$

$$[M] = \begin{bmatrix} M_{x1} & 0 & 0 & 0 & 0 & 0 \\ 0 & M_{y1} & 0 & 0 & 0 & 0 \\ 0 & 0 & M_{\theta1} & 0 & 0 & 0 \\ 0 & 0 & 0 & M_{x2} & 0 & 0 \\ 0 & 0 & 0 & 0 & M_{y2} & 0 \\ 0 & 0 & 0 & 0 & 0 & M_{\theta2} \end{bmatrix} \quad (5)$$

$$[M] = \begin{bmatrix} M_{x1} & 0 & 0 & 0 & 0 & 0 & 0 & 0 & 0 \\ 0 & M_{y1} & 0 & 0 & 0 & 0 & 0 & 0 & 0 \\ 0 & 0 & M_{\theta1} & 0 & 0 & 0 & 0 & 0 & 0 \\ 0 & 0 & 0 & M_{x2} & 0 & 0 & 0 & 0 & 0 \\ 0 & 0 & 0 & 0 & M_{y2} & 0 & 0 & 0 & 0 \\ 0 & 0 & 0 & 0 & 0 & M_{\theta2} & 0 & 0 & 0 \\ 0 & 0 & 0 & 0 & 0 & 0 & M_{x3} & 0 & 0 \\ 0 & 0 & 0 & 0 & 0 & 0 & 0 & M_{y3} & 0 \\ 0 & 0 & 0 & 0 & 0 & 0 & 0 & 0 & M_{\theta3} \end{bmatrix} \quad (6)$$

3. An external lever system to equivalent the corner lateral displacements

Using an MR damper in each floor of structure is not a cost-effective option, so in this article an external lever

system adopts to equivalent the corner lateral displacement. This system contains three levers, which connect to a solid member, and it connects to an MR damper with three levers. Finally, this controller device connects to a rigid structure. By using of this system, it is possible to equivalent the corner lateral displacement of each floor to a certain point. The general scheme of this system shows in Figs. 1-3. The main advantage of this system is decreasing the number of MR dampers for tall buildings by connecting every three floors with external levers to an MR damper.

4. MR damper models

4.1 Bingham plasticity model

This model is based on a parallel plate, which developed by Spencer *et al.* In the Bingham plasticity model, controlled and uncontrolled forces are generated. These forces obtained from Eqs. (7), (8), which in these equations $F_{controlled}$ is a controlled force and $F_{uncontrolled}$ is an uncontrolled force; w is the width of the rectangular plate; L is the effective axial pole length; h is the width of empty space between these plates; v_0 is the velocity and A_p is the cross-sectional area of piston (Tsang *et al.* 2006). Yang spent vast researches about the relation between controlled force and the intensity of the current. The relation between these forces and the intensity of current is presented in Eq. (9) (Yang 2001)

$$F_{uncontrolled} = F_{\eta} + F_f$$

$$F_{uncontrolled} = \left(1 + \frac{wh}{2A_p}\right) \frac{12\eta LA_p^2}{wh^3} v_0 + F_f \quad (7)$$

$$F_{Damper} = F_{controlled} + F_{\eta} + F_f$$

$$F_{controlled} = F_{Damper} - F_f - \left(1 + \frac{wh}{2A_p}\right) \frac{12\eta LA_p^2}{wh^3} v_0 \quad (8)$$

$$i(t) = \frac{1}{1.7} \ln\left(\frac{15.6 - F_{controlled}(t)}{16.4}\right) \quad (9)$$

4.2 The Bouc-Wen hysteresis model

The Bingham model is easy and useful for modeling an MR damper but it is not sufficient for illustrates the dynamic behavior of this device. Spencer *et al.* presented a new model for demonstrate the application of this device based on Bouc-Wen hysteresis model. In Bouc-Wen model, the total force of a damper is given by Eq. (10), which \dot{y} and \dot{z} are obtained from Eqs. (11), (12) (Tsang *et al.* 2006), Where y is the inner displacement of this device; x is the displacement of MR damper; z is the evolutionary variable, which illustrates the hysteric property; c_1 and c_0 are the viscous damping at low and high velocities; k_1 and k_0 are the accumulator stiffness and the stiffness at high velocities; x_0 is the initial displacement; α is the evolutionary coefficient; and A , n , β and γ are the shape

parameters of the hysteresis loop. According to the Yang's researches, some of these parameters can be obtained from Eqs. (13)-(15) (Yang 2001). Therefore, controlled and uncontrolled forces according to Bouc-Wen hysteresis method are obtained from Eqs. (16), (17)

$$F = \alpha z + c_0(\dot{x} - \dot{y}) + k_0(x - y) + k_1(x - x_0) = c_1\dot{y} + k_1(x - x_0) \quad (10)$$

$$\dot{y} = \frac{1}{c_0 + c_1} (\alpha z + c_0\dot{x} + k_0(x - y)) \quad (11)$$

$$\dot{z} = -\gamma |\dot{x} - \dot{y}| |z| |z|^{n-1} - \beta(\dot{x} - \dot{y}) |z|^n + A(\dot{x} - \dot{y}) \quad (12)$$

$$A = 2679m^{-1} \quad \beta = 647.46m^{-1} \quad \gamma = 647.46m^{-1} \quad n = 10$$

$$\alpha(i) = 16566i^3 - 87071i^2 + 168326i + 15114 \quad (13)$$

$$c_0(i) = 437097i^3 - 154540i^2 + 1641376i + 457741 \quad (14)$$

$$c_1(i) = -9363108i^3 + 5334183i^2 + 48788640i - 2791630 \quad (15)$$

$$F_{controlled} = \frac{c_1 \alpha z_u}{c_0 + c_1} + \frac{c_0 c_1}{c_0 + c_1} \quad (16)$$

$$F_{uncontrolled} = F_f \quad (17)$$

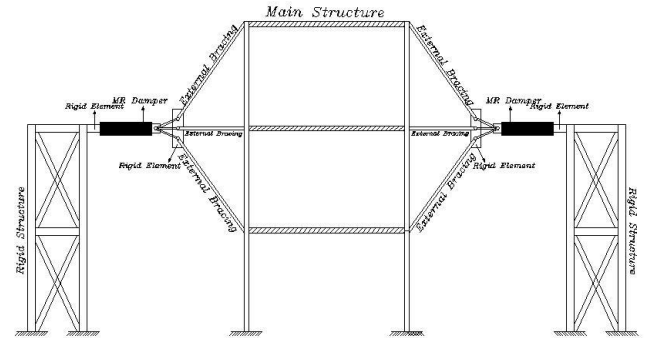


Fig. 1 Lever system and MR damper

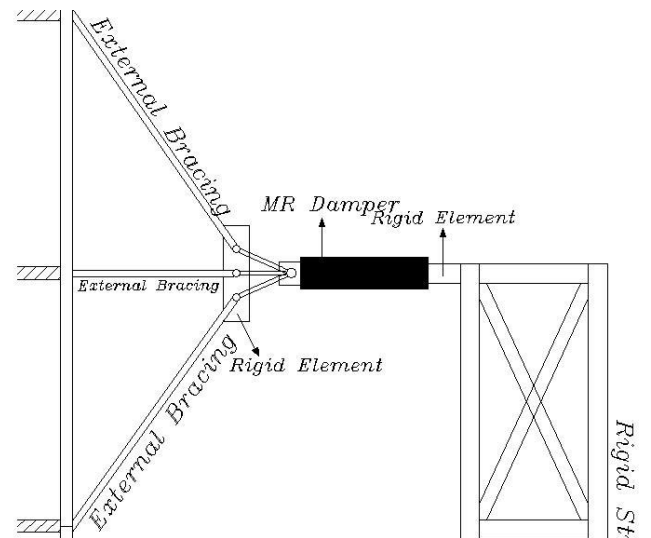


Fig. 2 Lever system and MR damper

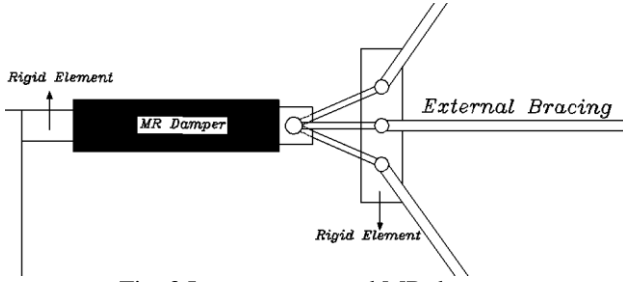


Fig. 3 Lever system and MR damper

Yang spent vast researches about the relation between controlled forces and intensity of the current in Bouc-Wen method. The relation between these parameters are presented in Eq. (18) (Yang 2001)

$$i(t) = \frac{1}{1.5} \ln\left(1 - \frac{F_{controlled}(t)}{1.5 \times 10^5}\right) \quad (18)$$

5. PID and Fuzzy logic algorithms

5.1 The PID algorithm

Generally, the proportional and Derivative controller caused to the steady state error, so the proportional-integral controller is used with the differentiator controller. This controller is called proportional-integral-derivative. The general form of PID controller is illustrated at Fig. (4) and the equation of this controller is shown at Eq. (19). There are different kind of methods for calculating the PID parameters such as, Ziegler-Nichols, Cohen Coon and etc. In this article the first method is used and the equations of this method are presented at Eqs. (20), (21) (Nigdeli 2014)

$$G(s) = K_p + K_d \cdot s + \frac{K_i}{s} \quad (19)$$

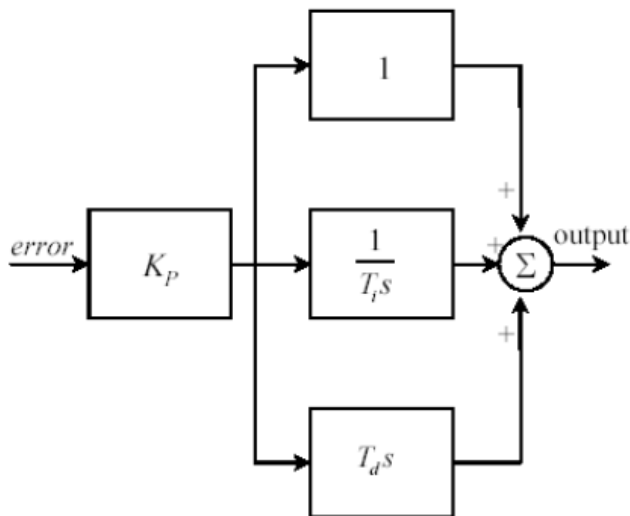


Fig. 4 The PID algorithm

$$G(s) = K_p \left(1 + T_d s + \frac{1}{T_i s}\right) = 0.6 \frac{T}{s} \left(s + \frac{1}{\tau_d}\right)^2 \quad (20)$$

$$G(s) = K_p \left(1 + T_d s + \frac{1}{T_i s}\right) = 0.075 \frac{K_{cr} P_{cr}}{s} \left(s + \frac{4}{P_{cr}}\right)^2$$

$$K_{cr} = K_p \quad \& \quad P_{cr} = \frac{2\pi}{\omega} \quad (21)$$

5.2 The fuzzy logic algorithm

The fuzzy logic controller is an approach to computing based on “degrees of truth” rather than the usual “true or false”. This idea was first advanced by Dr. Lotfi Zadeh of the University of California at Berkeley in the 1960s. Dr. Zadeh was working on the problem of computer understanding of natural language. The natural language is not easily translated into the absolute terms of true or false. Whether everything is ultimately describable in binary terms is a philosophical question worth pursuing, but in practice much data needed to feed a computer in some state in between and so, frequently, are the results of computing. One of the most common algorithms for controlling the structural response with using of MR damper is fuzzy algorithm. A sample of membership functions for fuzzy logic controller is presented in Fig. (5).

6. Numerical example

6.1 The structural properties

Here a three-floors building is considered with the

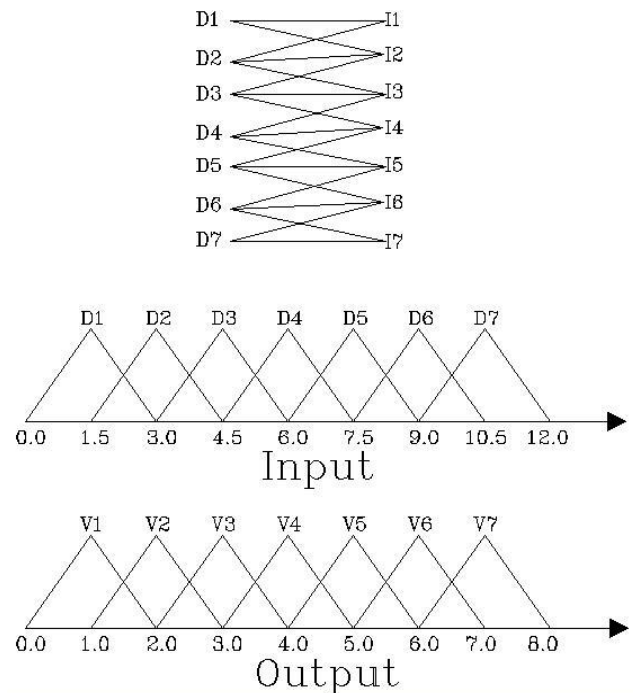


Fig. 5 The sample of input and output membership functions

dimension of 44 by 44 meters and eight earthquake records (Coalinga, Duzce, Imperial Valley, Kobe, San Fernando, Loma Prieta, Northridge and Wesmorland) are selected for this study. The transitional stiffness along x and y axis for the first, second and third floors are 3000 t/m , 2700 t/m and 2400 t/m and rotational stiffness is 95100 $t.m$. The total mass of each floor is 1360 t and rotational mass is 18200 $t.m^2$. The stiffness and mass matrices by assuming centrality of the center of mass for the calculations are according to Eqs. (22), (23).

6.2 The relation between an eccentricity and corner lateral displacement and damper forces

In this part, the damper forces and corner lateral displacements are presented for time-varying eccentricities. According to Figs. 6, 7 for all eight records of earthquake, by increasing an eccentricity of load, the average corner lateral displacement increases. The displacement can be increased from 6.1 centimeters for non eccentricity to 16.6 centimeters for maximum eccentricity in x direction and 6.15 centimeters to 17.1 centimeters in y axis. The performances, which consider for this structure are Immediate Occupancy(IO), Collapse Prevention(CP), Life Safety(LS), Damage Control Range(DCR) and Limited Safety Range(LSR). According to Figs. 8-10 by increasing the performance of structure and eccentricity, the damper forces increase. The amount of damper forces increase from 5.6 tons for non-eccentricity to 149 tons for maximum ones in x direction and 4.5 to 140 tons in y direction. The response for Loma Prieta and Northridge records show higher values. In Figs. 11, 12 the relation between an eccentricity and damper forces for all performances are illustrated for Northridge earthquake. In these diagrams when the corner lateral displacement are less than the target displacement for any performance, the damper force is equal to zero. The comparison between controlled and uncontrolled response of structure for the 1.8 meters eccentricity value with Elcentro record shows at Fig. 13, which illustrates that using MR damper for mitigation the structural response is so effective

$$[K] = \begin{bmatrix} K_{11} & K_{12} & K_{13} & K_{14} & K_{15} & K_{16} & K_{17} & K_{18} & K_{19} \\ K_{21} & K_{22} & K_{23} & K_{24} & K_{25} & K_{26} & K_{27} & K_{28} & K_{29} \\ K_{31} & K_{32} & K_{33} & K_{34} & K_{35} & K_{36} & K_{37} & K_{38} & K_{39} \\ K_{41} & K_{42} & K_{43} & K_{44} & K_{45} & K_{46} & K_{47} & K_{48} & K_{49} \\ K_{51} & K_{52} & K_{53} & K_{54} & K_{55} & K_{56} & K_{57} & K_{58} & K_{59} \\ K_{61} & K_{62} & K_{63} & K_{64} & K_{65} & K_{66} & K_{67} & K_{68} & K_{69} \\ K_{71} & K_{72} & K_{73} & K_{74} & K_{75} & K_{76} & K_{77} & K_{78} & K_{79} \\ K_{81} & K_{82} & K_{83} & K_{84} & K_{85} & K_{86} & K_{87} & K_{88} & K_{89} \\ K_{91} & K_{92} & K_{93} & K_{94} & K_{95} & K_{96} & K_{97} & K_{98} & K_{99} \end{bmatrix} \quad (22)$$

$$\begin{aligned} K_{11} &= 5700, & K_{12} &= 0, & K_{13} &= -3000e_{y1} - 2700e_{y1}, & K_{14} &= -2700 \\ K_{15} &= 0, & K_{16} &= 2700e_{y2}, & K_{17} &= 0, & K_{18} &= 0, & K_{19} &= 0 \\ K_{21} &= 0, & K_{22} &= 5700, & K_{23} &= 3000e_{x1} + 2700e_{x1}, & K_{24} &= 0, & K_{25} &= -2700 \\ K_{26} &= -2700e_{x2}, & K_{27} &= 0, & K_{28} &= 0, & K_{29} &= 0 \end{aligned}$$

$$\begin{aligned} K_{31} &= -3000e_{y1} - 2700e_{y1}, & K_{32} &= 3000e_{x1} + 2700e_{x1} \\ K_{33} &= 95100 + 3000e_{y1}^2 + 3000e_{x1}^2 + 2700e_{y1}^2 + 2700e_{x1}^2 \\ K_{34} &= 2700e_{y1}, & K_{35} &= -2700e_{x1}, & K_{36} &= -2700e_{y1}e_{y2} - 2700e_{x1}e_{x2} \\ K_{37} &= 0, & K_{38} &= 0, & K_{39} &= 0 \\ K_{41} &= -2700, & K_{42} &= 0, & K_{43} &= 2700e_{y1} \\ K_{44} &= 5100, & K_{45} &= 0, & K_{46} &= -2700e_{y2} - 2400e_{y2} \\ K_{47} &= -2400, & K_{48} &= 0, & K_{49} &= 2400e_{y3} \\ \\ K_{51} &= 0, & K_{52} &= -2700, & K_{53} &= -2700e_{x1} \\ K_{54} &= 0, & K_{55} &= 5100, & K_{56} &= 2700e_{x2} + 2400e_{x2} \\ K_{57} &= 0, & K_{58} &= -2400, & K_{59} &= -2400e_{x3} \\ K_{61} &= 2700e_{y2}, & K_{62} &= -2700e_{x2}, & K_{63} &= -2700e_{y1}e_{y2} - 2700e_{x1}e_{x2} \\ K_{64} &= -2700e_{y2} - 2400e_{y2}, & K_{65} &= 2700e_{x2} + 2400e_{x2} \\ K_{66} &= 95100 + 2700e_{y2}^2 + 2400e_{y2}^2 + 2700e_{x2}^2 + 2400e_{x2}^2 \\ K_{67} &= 2400e_{y2}, & K_{68} &= -2400e_{x2}, & K_{69} &= -2400e_{y2}e_{y3} - 2400e_{x2}e_{x3} \\ \\ K_{71} &= 0, & K_{72} &= 0, & K_{73} &= 0 \\ K_{74} &= -2400, & K_{75} &= 0, & K_{76} &= 2400e_{y2} \\ K_{77} &= 2400, & K_{78} &= 0, & K_{79} &= -2400e_{y3} \\ K_{81} &= 0, & K_{82} &= 0, & K_{83} &= 0 \\ K_{84} &= 0, & K_{85} &= -2400, & K_{86} &= -2400e_{x2} \\ K_{87} &= 0, & K_{88} &= 2400, & K_{89} &= 2400e_{x3} \\ K_{91} &= 0, & K_{92} &= 0, & K_{93} &= 0 \\ K_{94} &= 2400e_{y3}, & K_{95} &= -2400e_{x3}, & K_{96} &= -2400e_{y2}e_{y3} - 2400e_{x2}e_{x3} \\ K_{97} &= -2400e_{y3}, & K_{98} &= 2400e_{x3}, & K_{99} &= 95100 + 2400e_{y3}^2 + 2400e_{x3}^2 \end{aligned}$$

$$[M] = \begin{bmatrix} 13.6 & 0 & 0 & 0 & 0 & 0 & 0 & 0 & 0 \\ 0 & 13.6 & 0 & 0 & 0 & 0 & 0 & 0 & 0 \\ 0 & 0 & 182 & 0 & 0 & 0 & 0 & 0 & 0 \\ 0 & 0 & 0 & 13.6 & 0 & 0 & 0 & 0 & 0 \\ 0 & 0 & 0 & 0 & 13.6 & 0 & 0 & 0 & 0 \\ 0 & 0 & 0 & 0 & 0 & 182 & 0 & 0 & 0 \\ 0 & 0 & 0 & 0 & 0 & 0 & 13.6 & 0 & 0 \\ 0 & 0 & 0 & 0 & 0 & 0 & 0 & 13.6 & 0 \\ 0 & 0 & 0 & 0 & 0 & 0 & 0 & 0 & 182 \end{bmatrix} \times 10^2 \quad (23)$$

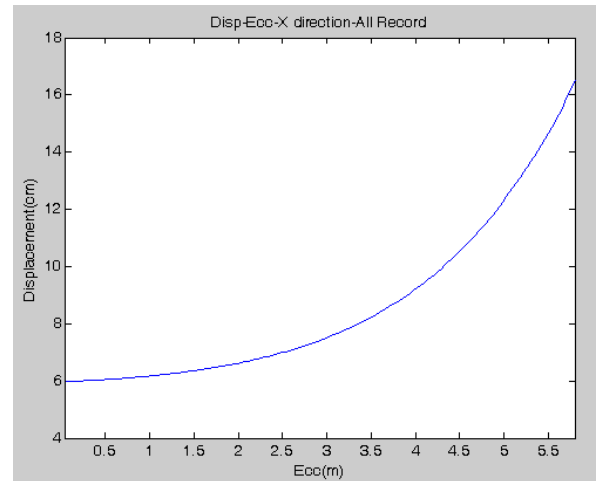


Fig. 6 The relation between an eccentricity and average corner lateral displacement along x axis

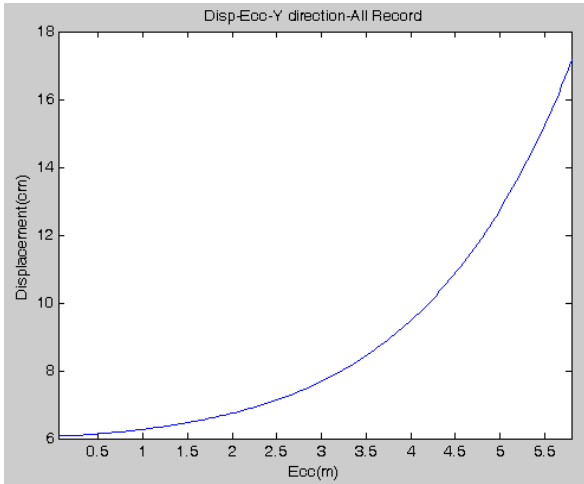


Fig. 7 The relation between an eccentricity and average corner lateral displacement along y axis

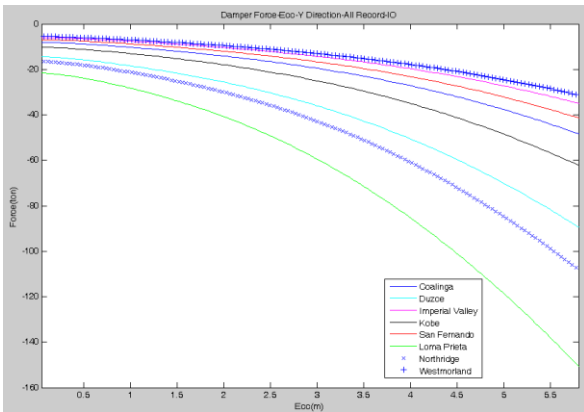


Fig. 8 The relation between an eccentricity and damper force for IO performance-PID controller

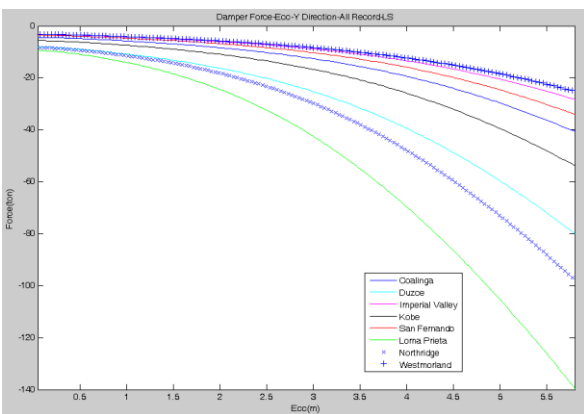


Fig. 9 The relation between an eccentricity and damper force for LS performance-PID controller

6.3 Comparison between Bingham and Bouc-Wen's methods

The damper forces in these methods are so close, infact in some cases they are coincident, but the intensity of current is completely different. Figs. 13-18 show the comparison between the average damper forces and the intensity of current of these methods for all eight records of

earthquake. In Bouc-Wen's method it increases initially then decreases and after that increases smoothly, but in Bingham's method it just increases. Therefore, in Bouc-

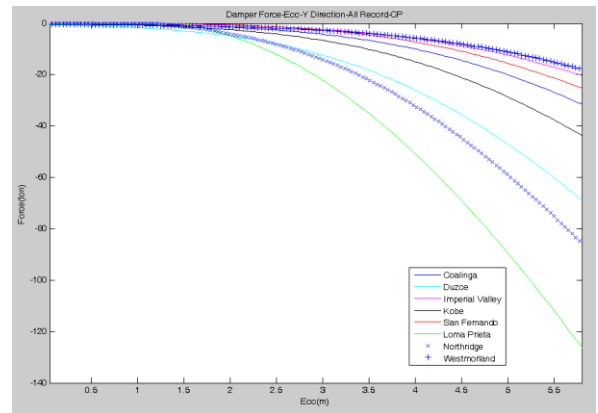


Fig. 10 The relation between an eccentricity and damper force for CP performance-PID controller

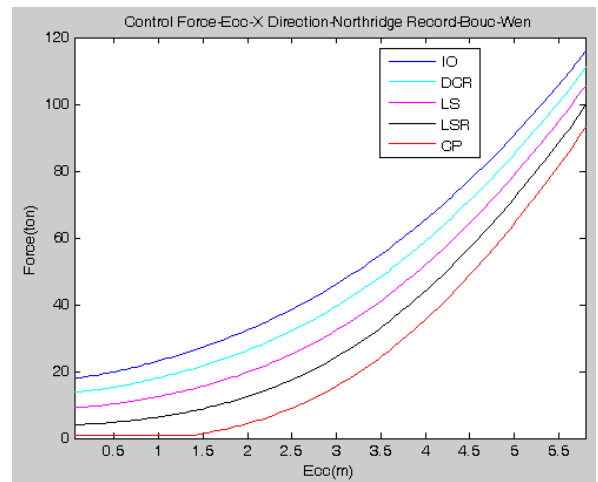


Fig. 11 The relation between an eccentricity and damper force for Northridge earthquake for all performances along x axis-PID controller

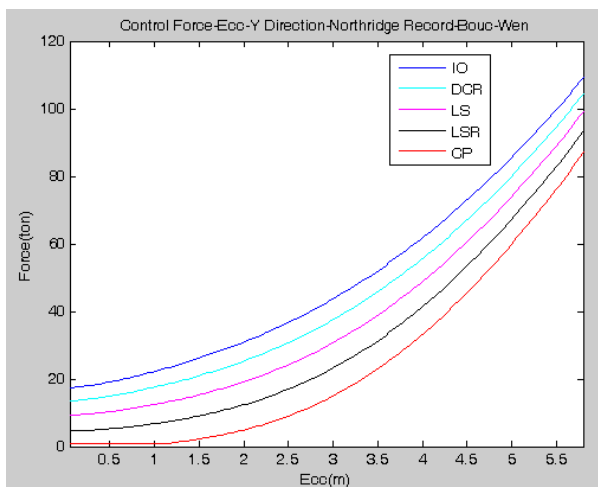


Fig. 12 The relation between an eccentricity and damper force for Northridge earthquake for all performances along y axis-PID controller

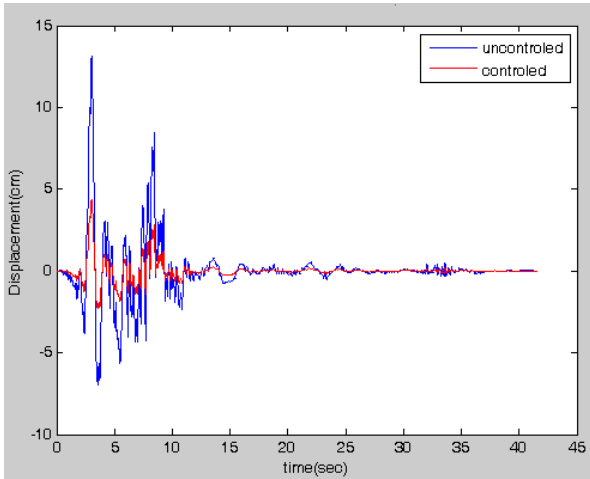


Fig. 13(a) The comparison between controlled and uncontrolled response of structure for Elcentro earthquake by using of PID controller

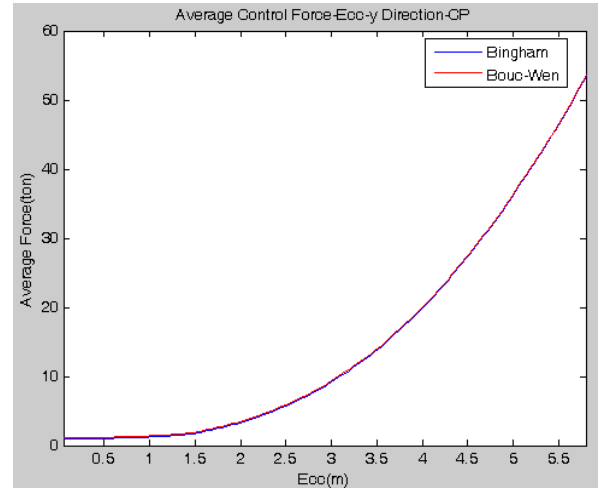


Fig. 15 The relation between an eccentricity and average damper force for 8 records of earthquake for CP performance-PID controller

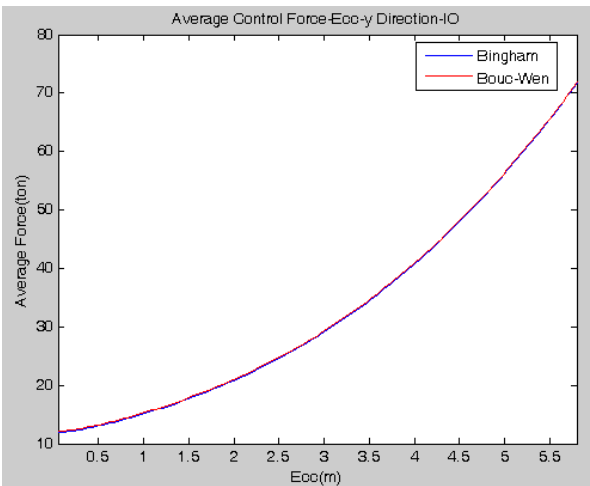


Fig. 13(b) The relation between an eccentricity and average damper force for 8 records of earthquake for IO performance-PID controller

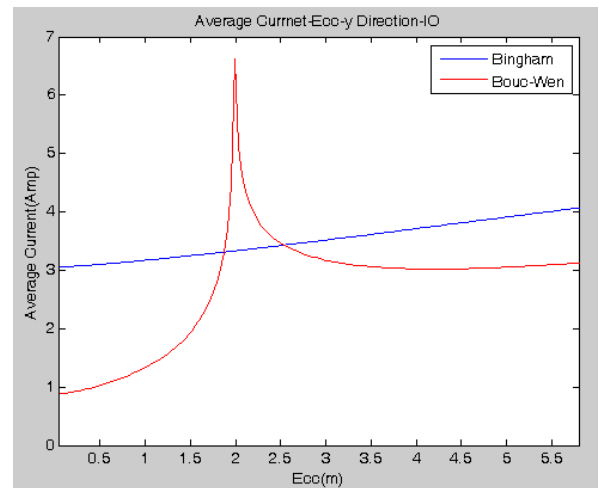


Fig. 16 The relation between an eccentricity and average current for 8 records of earthquake for IO performance-PID controller

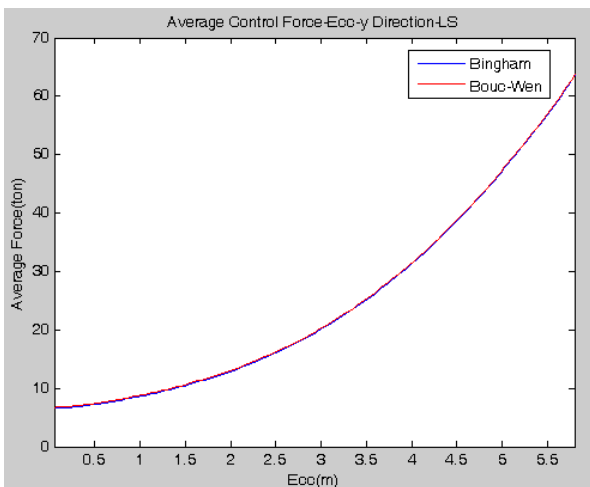


Fig. 14 The relation between an eccentricity and average damper force for 8 records of earthquake for LS performance-PID controller

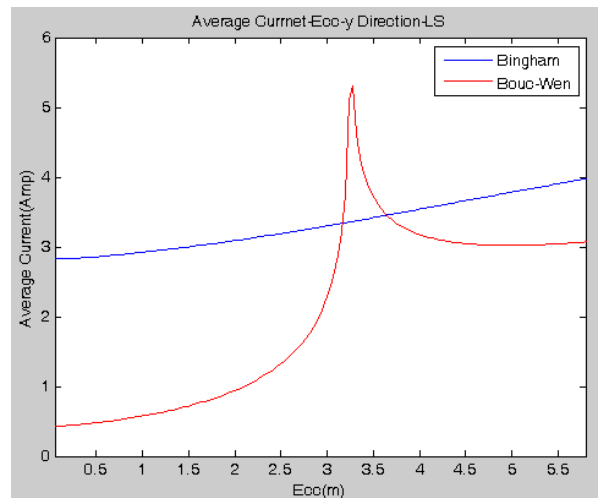


Fig. 17 The relation between an eccentricity and average current for 8 records of earthquake for LS performance-PID controller

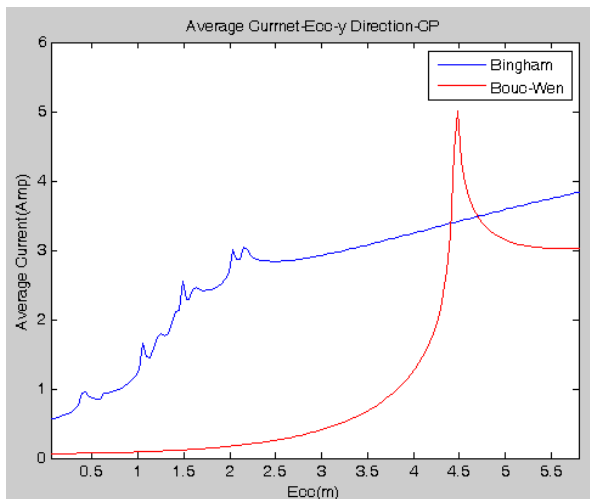


Fig. 18 The relation between an eccentricity and average current for 8 records of earthquake for CP performance-PID controller

Wen's method, the main reason of this phenomenon is that by increasing an eccentricity of load the uncontrolled forces increase and controlled forces decrease. In these diagrams when the corner lateral displacement is less than the target displacement for any performances, the intensity of current is equal to zero. The required power supply for both methods is very low, but its influence for reduction the structural response is significant.

7. Conclusions

This article was all about controlling the corner lateral displacement of structure with an external lever system by using of MR damper with PID control algorithm. In this paper, the Bingham and Bouc-Wen's methods were utilized, and the results illustrated that the value of controlled force for each method was so close together, but the intensities of the current algorithms were completely different from each other. The amount of power supply for this system is very low, but it can decrease the corner lateral displacement, significantly. This system can be used for particular structure like as nuclear power plant, governmental and military structures and etc., and it must have enough space around the structure to locate levers, MR dampers and rigid structure. So, using this method for controlling the corner lateral displacement of structure for both torsional and transitional deflection of building can be very useful and the safety of structure will be guaranteed, because an eccentricity can be changed during an earthquake.

References

- Bahmani, P., van de Lindt, J. and Dao, T.N. (2014), "Displacement-based design of buildings with torsion: Theory and verification", *J. Struct. Eng.*, ASCE, **140**(6), 267-280.
- Carlson, J. and Spencer, B. (1996), "Magnetorheological fluid dampers for semi-active control", *Proceedings of the 3rd International Conference on Motion and Vibration Control*, **3**,

35-40.

- Ghasemi, M.R. and Barghi, E. (2012), "Estimation of inverse dynamic behavior of MR dampers using artificial and fuzzy-based neural networks", *Int. J. Optimiz. Civ. Eng.*, **2**(3), 357-368.
- Kamatchi P., Ramana G.V., Nagpal A.K., Iyer N.R. and Bhat J.A. (2015), "Dynamic to static eccentricity ratio for site-specific earthquakes", *Earthq. Struct.*, **9**(2), 391-413.
- Kevadkar, M.D. and Kodag, P.B. (2013), "Lateral load analysis of R.C.C. building", *Int. J. Modern Eng. Res.*, **3**(3), 1428-1434.
- Mousaad, A. (2013), "Vibration control of buildings using magnetorheological damper: A new control algorithm", *J. Eng.*, Hindawi Publishing Corporation, doi: 10.1155/2013/596078.
- Nigdeli, S.M. (2014), "Effect of feedback on PID controlled active structures under earthquake excitations", *Earthq. Struct.*, **6**(2), 1171-1186.
- Serror, M.H., Diab, R.A. and Mourad, S.A. (2014), "Seismic force reduction factor for steel moment resisting frames with supplemental viscous dampers", *Earthq. Struct.*, **7**(6), 1171-1186.
- Spencer, B., Dyke, S., Sain, M. and Carlson, J. (1996), "Seismic response reduction using magnetorheological dampers", *Proceedings of the IFAC World Congress*, San Francisco, CA.
- Spencer, B., Dyke, S., Sain, M. and Carlson, J. (1998), "An experimental study of MR dampers for seismic protection", *Smart Mater. Struct.*, **7**(5), 693-703.
- Spencer, B., Dyke, S., Sain, M. and Carlson, J. (1996), "Experimental verification of semi-active control strategies using acceleration feedback", *Proceedings of 3rd International Conference on Motion and Vibration Control*, **3**, 291-296.
- Spencer, B., Dyke, S., Sain, M. and Carlson, J. (1996), "Modeling and control of magnetorheological dampers for seismic response reduction", *Smart Mater. Struct.*, **5**(5), 565-575.
- Spencer, B., Dyke, S., Sain, M. and Carlson, J. (1997), "Phenomenological model for magnetorheological dampers", *J. Eng. Mech.*, ASCE, **123**(3), 230-238.
- Spencer, B., Yang, G., Carlson, J. and Sain, M. (1998), "Smart dampers for seismic protection of structures: a full-scale study", *Proceeding of the 2nd World Conference on Structural Control*, Kyoto, Japan.
- Spencer, B., Yang, G., Carlson, J. and Sain, M. (2002), "Large-scale MR fluid dampers: modeling and dynamic performance considerations", *Eng. Struct.*, **24**(3), 309-323.
- Stathi, C.G., Bakas, N.P., Lagaros, N.D. and Papadrakakis, M. (2015), "Ratio of Torsion (ROT): An index for assessing the global induced torsion in plan irregular buildings", *Earthq. Struct.*, **9**(1), 145-171.
- Tsang, H.H., Su, K. and Chandler, A. (2006), "Simplified inverse dynamics models for MR fluid dampers", *Eng. Struct.*, **28**(3), 327-341.
- Yang, G. (2001), "Large-scale magnetorheological fluid damper for vibration mitigation: Modeling, testing and control", Ph.D. dissertation, University of Notre Dame.
- Zadeh, L.A. (1965), "Fuzzy sets", *Inform. Control.*, **8**(3), 338-353.

CC